Materials Physics and Mechanics. 2023;51(4):160-171
Research article
http://dx.doi.org/10.18149/MPM.5142023_14

Submitted: October 30, 2022
Approved: February 7, 2023
Accepted: May 12, 2023

Simulation of the stress-strain state of a rectangular bar using fast trigonometric interpolation in various statements of boundary value problems

A.D. Chernyshov [1], V.V. Goryainov [2] ✉, E.N. Kovaleva [1]

[1] Voronezh State University of Engineering Technology, Voronezh, Russia

[2] Voronezh State Technical University, Voronezh, Russia

✉ gorvit77@mail.ru

Abstract. The problem of stresses in a rectangular bar is considered in three statements: 1) with assignment on all boundaries of displacements, 2) stresses and 3) with mixed boundary conditions. The solution is represented by a fast expansion whose coefficients were determined by fast trigonometric interpolation. The solution of the boundary value problem with Dirichlet conditions is the most accurate of the three considered boundary value problems. Compared with this problem, the accuracy of determining the components of the stress tensor and the residual of the Lamé equations in the other two boundary value problems drops by an order of magnitude. The largest residual of the Lamé equilibrium equations is observed in the boundary value problem with given stresses on all sides of the rectangle. Computational experiments showed that the aspect ratio of the rectangle affects the qualitative form of the stress intensity distribution and the location of points with the maximum stress intensity. Among all rectangular sections with different overall dimensions, but the same sectional area, the smallest value of $\tilde{\sigma}_{max}$ is observed in a bar with a square section.

Keywords: displacements; stress tensor components; Lamé equations; fast expansions; fast trigonometric interpolation; boundary value problems; high accuracy

Citation: Chernyshov AD, Goryainov VV, Kovaleva EN. Simulation of the stress-strain state of a rectangular bar using fast trigonometric interpolation in various statements of boundary value problems. *Materials Physics and Mechanics.* 2023;51(4): 160-171. DOI: 10.18149/MPM.5142023_14.

Introduction

A rectangular region is one of the simplest two-dimensional regions for which it is convenient to model the stress-deformed state of a material and consider its properties [1–10]. Approximate solutions for similar object shapes are obtained by various numerical and analytical methods. Thus, in [1], an approximate analytical solution in the form of trigonometric polynomials is constructed by the superposition method from two solutions obtained by the method of initial functions. In [2,9], solutions are presented as series in Papkovich–Fadle eigenfunctions. In [4], the solution is sought as the sum of a trigonometric series and a power function with a root singularity. The superposition method in the form of Fourier series satisfying the differential equation and boundary conditions is used in [5]. Finite difference and finite element methods were used in [3,8], respectively. Unknown displacements in [11] are represented by power series. In [12], the integral Fourier transform with respect to a variable running through an infinite interval was used. For problems of rigid

Publisher: Peter the Great St. Petersburg Polytechnic University

body mechanics, the nodal integration method for meshfree radial point interpolation is presented in [13]. In the proposed method, radial basis functions supplemented by polynomials are used to construct shape functions that have the delta function property. In [14], a grid method is presented using a special trigonometric basis; the completeness of the trigonometric basis is not discussed. The grid method of collocations and least squares for the residual, applicable in solving multidimensional nonlinear problems of elliptic type, was proposed in [15]. Interpolation methods were used to process the experimental data [16] and to determine the plasticity and creep characteristics of the material [17]. The exact solutions presented in [18] were obtained using group analysis for an elastic model written in Euler variables at finite strains, and in [10], the exact solutions for deflections of a rectangular membrane under the action of a variable load were obtained by the method of fast expansions. The method of fast expansions was developed in [19]. It is based on the fact that the desired solution of the problem is represented as the sum of a special boundary function and a Fourier series. Such a sum is called a fast expansion. Unknown coefficients of fast expansion are found using the operator of fast expansions [20] or fast trigonometric interpolation [21]. The use of classical trigonometric interpolation to determine the coefficients of fast expansion is problematic due to the impossibility of its differentiation in the general case and the large error between interpolation points. Therefore, classical trigonometric interpolation is usually used to solve problems not related to integro-differential equations, for example, to improve the quality of image processing [22] and restore periodic discrete signals of finite duration [23].

In this paper, we present the solution of the problem of stresses in a bar by the method of fast expansions in three statements. They differ from each other in the type of boundary conditions. The coefficients of fast expansions will be determined using fast trigonometric interpolation. In this regard, it is of interest to study the influence of the type of boundary conditions on the accuracy of solving the problem using fast trigonometric interpolation.

Methods

Under conditions of plane deformation, the projections of the displacements vector of the bar material points depend only on the coordinates x, y:

$$U = U(x, y),\ V = V(x, y),\ W = 0. \tag{1}$$

The stress tensor components will have the following form:

$$\sigma_{xx} = (\lambda + 2\mu)\frac{\partial U}{\partial x} + \lambda\frac{\partial V}{\partial y},\quad \sigma_{yy} = (\lambda + 2\mu)\frac{\partial V}{\partial y} + \lambda\frac{\partial U}{\partial x},$$
$$\tau_{xy} = \mu\left(\frac{\partial U}{\partial y} + \frac{\partial V}{\partial x}\right),\ \sigma_{zz} = \lambda\left(\frac{\partial U}{\partial x} + \frac{\partial V}{\partial y}\right),\quad \tau_{xz} = \tau_{yz} = 0. \tag{2}$$

Let us write the Lamé equilibrium equations for displacements taking into account mass forces

$$(\lambda + 2\mu)\frac{\partial^2 U}{\partial x^2} + (\lambda + \mu)\frac{\partial^2 V}{\partial x \partial y} + \mu\frac{\partial^2 U}{\partial y^2} + X(x, y) = 0, \tag{3}$$

$$(\lambda + 2\mu)\frac{\partial^2 V}{\partial y^2} + (\lambda + \mu)\frac{\partial^2 U}{\partial x \partial y} + \mu\frac{\partial^2 V}{\partial x^2} + Y(x, y) = 0. \tag{4}$$

We add boundary conditions to equations (3), (4). We assume that the elastic bar has a rectangular cross-section $\Omega = (0 \le x \le a,\ 0 \le y \le b)$. On the sides of the bar, we set three different types of boundary conditions, corresponding to three boundary value problems.

1. Displacements are given on all sides

$$U|_{x=0} = f_1(y),\ U|_{x=a} = f_3(y),\ V|_{x=0} = \varphi_1(y),\ V|_{x=a} = \varphi_3(y). \tag{5}$$

$$U\big|_{y=0} = f_2(x),\ U\big|_{y=b} = f_4(x),\ V\big|_{y=0} = \varphi_2(x),\ V\big|_{y=b} = \varphi_4(x). \tag{6}$$

2. Stresses are set on all sides

$$(\lambda+2\mu)\frac{\partial U}{\partial x}+\lambda\frac{\partial V}{\partial y}\bigg|_{x=0} = F_1(y),\ \ \mu\left(\frac{\partial U}{\partial y}+\frac{\partial V}{\partial x}\right)\bigg|_{x=0} = \Phi_1(y), \tag{7}$$

$$(\lambda+2\mu)\frac{\partial U}{\partial x}+\lambda\frac{\partial V}{\partial y}\bigg|_{x=a} = F_2(y),\ \ \mu\left(\frac{\partial U}{\partial y}+\frac{\partial V}{\partial x}\right)\bigg|_{x=a} = \Phi_2(y). \tag{8}$$

$$(\lambda+2\mu)\frac{\partial V}{\partial y}+\lambda\frac{\partial U}{\partial x}\bigg|_{y=b} = F_3(x),\ \ \mu\left(\frac{\partial U}{\partial y}+\frac{\partial V}{\partial x}\right)\bigg|_{y=b} = \Phi_3(x), \tag{9}$$

$$(\lambda+2\mu)\frac{\partial V}{\partial y}+\lambda\frac{\partial U}{\partial x}\bigg|_{y=0} = F_4(x),\ \ \mu\left(\frac{\partial U}{\partial y}+\frac{\partial V}{\partial x}\right)\bigg|_{y=0} = \Phi_4(x). \tag{10}$$

3. Mixed boundary conditions are on the sides $x=0$, $x=a$ and $y=b$. We set the stresses in the form (7), (8) and (9), respectively, and on the side we set the displacements

$$U\big|_{y=0} = g_1(x),\ \ V\big|_{y=0} = g_2(x). \tag{11}$$

The functions included in the boundary conditions (5) – (10) should be selected taking into account the matching conditions. So, for the case of specifying displacements on all boundaries of the rectangle, the matching conditions have the form

$$\begin{aligned} &f_1(0)=f_2(0)\ ,\ f_3(0)=f_2(a)\ ,\ f_3(b)=f_4(a)\ ,\ f_4(0)=f_1(b),\\ &\varphi_1(0)=\varphi_2(0)\ ,\ \varphi_3(0)=\varphi_2(a)\ ,\ \varphi_3(b)=\varphi_4(a)\ ,\ \varphi_4(0)=\varphi_1(b). \end{aligned} \tag{12}$$

In the case of specifying stresses at all boundaries, we write the matching conditions for shear stresses as follows

$$\Phi_4(0)=\Phi_1(0)\ ,\ \Phi_3(0)=\Phi_1(b)\ ,\ \Phi_3(a)=\Phi_2(b),\ \Phi_4(a)=\Phi_2(0). \tag{13}$$

For the mixed boundary conditions specified in the third paragraph, the matching conditions are as follows

$$\Phi_3(0)=\Phi_1(b)\ ,\ \Phi_3(a)=\Phi_2(b). \tag{14}$$

Compliance with the matching conditions will allow finding a continuous solution to three problems: 1. (3) – (6); 2. (3), (4), (7) – (10); 3. (3), (4), (7) – (9), (11).

As an example of the function from (5) – (11), we set as follows

$$\begin{aligned} &f_1(y)=0,\ \ f_2(x)=0,\ \ f_3(y)=K\sin 1.2\pi a y,\ \ f_4(x)=K\sin 1.2\pi b x,\\ &\varphi_1(y)=0,\ \ \varphi_2(x)=0,\ \ \varphi_3(x)=-K\sin a\sin y,\ \ \varphi_4(x)=-K\sin x\sin b. \end{aligned} \tag{15}$$

$$\begin{aligned} &g_1(x)=g_2(x)=0.\\ &F_1(y)=1.2\pi K(\lambda+2\mu)\,y\cos 1.2\pi a y,\quad \Phi_1(y)=-\mu K\sin y,\\ &F_2(y)=1.2\pi K(\lambda+2\mu)\,y\cos 1.2\pi a y-\lambda K\sin a\cos y,\\ &\Phi_2(y)=\mu\left(-K\cos a\sin y+1.2\pi K a\cos 1.2 a y\right),\\ &F_3(y)=-K(\lambda+2\mu)\sin x\cos b+1.2\pi\lambda K b\cos 1.2\pi x b,\\ &\Phi_3(y)=\mu\left(-K\cos x\sin b+1.2\pi K x\cos 1.2 x b\right),\\ &F_4(y)=-K(\lambda+2\mu)\sin x,\ \Phi_4(y)=1.2\pi\mu K x, \end{aligned} \tag{16}$$

We write the mass forces in (3), (4) by the expressions

$$\begin{aligned} X(x,y) &= (1.2\pi y)^2(\lambda+2\mu)K\sin 1.2\pi xy + \\ &+(\lambda+\mu)K\cos x\cos y+(1.2\pi x)^2\mu K\sin 1.2\pi xy, \\ Y(x,y) &= -(\lambda+2\mu)K\sin x\sin y-\mu K\sin x\sin y + \\ &+(\lambda+\mu)\left((1.2\pi)^2 xyK\sin 1.2\pi xy-1.2\pi K\cos 1.2\pi xy\right). \end{aligned} \quad (17)$$

Dependencies (15) – (17) are chosen so that each of the three boundary value problems (1. (3) – (6); 2. (3), (4), (7) – (10); 3. (3), (4), (7) – (9), (11)) had the exact solution

$$U(x,y)=K\sin 1.2\pi xy,\ V(x,y)=-K\sin x\sin y, \quad (18)$$

where K is a constant that controls the amount of displacement.

The exact solution (18) will allow us to study the error in solving three boundary value problems by comparing it with an approximate analytical solution obtained by the fast expansion method. In the comparison, the following will be calculated: the relative error of the stress tensor components (2), the residual of the Lamé equilibrium equations (3), (4) and the residual of the boundary conditions (5) – (11).

Let us show in detail the solution of one of the three boundary value problems, for example, for the case of specifying displacements on all sides of a rectangle. For the other two boundary value problems, we note the distinctive features in the process of the solution.

For the solution, we will use the approximate analytical method of fast sine expansions [1], according to which we represent $U=U(x,y)$ and $V=V(x,y)$ as the sum of the 6th order boundary functions $M_6^U(x;y)$, $M_6^V(x;y)$ and the Fourier series in sines

$$\begin{aligned} U &= M_6^U(x;y)+\sum_{m=1}^{N_1}u_m(x)\sin m\pi\frac{y}{b}, \\ V &= M_6^V(x;y)+\sum_{m=1}^{N_1}\upsilon_m(x)\sin m\pi\frac{y}{b},\ x\in[0;a],\ y\in[0;b]. \end{aligned} \quad (19)$$

Here, N_1 – is the number of terms taken in the Fourier series. The boundary functions $M_6^U(x;y)$ and $M_6^V(x;y)$ of the sixth order are defined by the equalities

$$M_6^U(x;y)=\sum_{i=1}^{8}A_i(x)P_i(y),\ M_6^V(x;y)=\sum_{i=1}^{8}B_i(x)P_i(y), \quad (20)$$

where $A_i(x)$ и $B_i(x)$, $i=1\div 8$ are the coefficients of boundary functions, $P_i(y)$, $i=1\div 8$ – fast polynomials [1].

Fast polynomials $P_i(y)$ and coefficients $A_i(x)$, $B_i(x)$ are defined by the equalities:

$$P_1(y)=\left(1-\frac{y}{b}\right),\ P_2(y)=\frac{y}{b},\ P_3(y)=\left(\frac{y^2}{2}-\frac{y^3}{6b}-\frac{by}{3}\right),\ P_4(x)=\left(\frac{y^3}{6b}-\frac{by}{6}\right),$$

$$P_5(y)=\left(\frac{y^4}{24}-\frac{y^5}{120b}-\frac{by^3}{18}+\frac{b^3y}{45}\right),\ P_6(y)=\left(\frac{y^5}{120b}-\frac{by^3}{36}+\frac{7b^3y}{360}\right),$$

$$P_7(y)=\left(\frac{y^6}{720}-\frac{y^7}{5040b}-\frac{by^5}{360}+\frac{b^3y^3}{270}-\frac{2b^5y}{945}\right),$$

$$P_8(y)=\left(\frac{y^7}{5040b}-\frac{by^5}{720}+\frac{7b^3y^3}{2160}-\frac{31b^5y}{15120}\right).$$

$$A_1(x)=U\big|_{y=0},\ A_2(x)=U\big|_{y=a},\ A_3(x)=\left.\frac{\partial^2 U}{\partial y^2}\right|_{y=0},\ A_4(x)=\left.\frac{\partial^2 U}{\partial y^2}\right|_{y=a},$$
$$A_5(x)=\left.\frac{\partial^4 U}{\partial y^4}\right|_{y=0},\ A_6(x)=\left.\frac{\partial^4 U}{\partial y^4}\right|_{y=a},\ A_7(x)=\left.\frac{\partial^6 U}{\partial y^6}\right|_{y=0},\ A_8(x)=\left.\frac{\partial^6 U}{\partial y^6}\right|_{y=a},$$
$$B_1(x)=V\big|_{y=0},\ B_2(x)=V\big|_{y=a},\ B_3(x)=\left.\frac{\partial^2 V}{\partial y^2}\right|_{y=0},\ B_4(x)=\left.\frac{\partial^2 V}{\partial y^2}\right|_{y=a},$$
$$B_5(x)=\left.\frac{\partial^4 V}{\partial y^4}\right|_{y=0},\ B_6(x)=\left.\frac{\partial^4 V}{\partial y^4}\right|_{y=a},\ B_7(x)=\left.\frac{\partial^6 V}{\partial y^6}\right|_{y=0},\ B_8(x)=\left.\frac{\partial^6 V}{\partial y^6}\right|_{y=a}. \quad (21)$$

To be able to execute expressions (21), it is necessary that $U=U(x,y)$ and $V=V(x,y)$ satisfy the smoothness condition $(U,V)\in C^{(6)}(\Omega)$.

The unknowns in (19) are functions that depend on only one variable *x*:

$$A_1(x)\div A_8(x),\ B_1(x)\div B_8(x),\ u_m(x),\ \upsilon_m(x),\ m=1...N_1. \quad (22)$$

We represent the functions from (22) by fast expansions in *x*. Moreover, in these repeated expansions, boundary functions of the same orders are used as in fast expansions (19) in the variable *y*:

$$A_i(x)=M_6^{A(i)}(x)+\sum_{n=1}^{N_2}a_{n+8}^{(i)}\sin n\pi\frac{x}{a},\ B_i(x)=M_6^{B(i)}(x)+\sum_{n=1}^{N_2}b_{n+8}^{(i)}\sin n\pi\frac{x}{a},$$
$$u_m(x)=M_6^{u(m)}(x)+\sum_{n=1}^{N_2}u_{n+8}^{(m)}\sin n\pi\frac{x}{a},\ \upsilon_m(x)=M_6^{\upsilon(m)}(x)+\sum_{n=1}^{N_2}\upsilon_{n+8}^{(m)}\sin n\pi\frac{x}{a}, \quad (23)$$
$$i=1...8,\ m=1...N_1.$$

In (23), N_2 – denotes the number of terms taken into account in the Fourier series. Boundary functions $M_6^{A(i)}(x),\ M_6^{B(i)}(x),\ M_6^{u(m)}(x),\ M_6^{\upsilon(m)}(x)$ are defined by equalities

$$M_6^{A(i)}(x)=\sum_{k=1}^{8}a_k^{(i)}P_k(x),\ M_6^{B(i)}(x)=\sum_{k=1}^{8}b_k^{(i)}P_k(x),$$
$$M_6^{u(m)}(x)=\sum_{k=1}^{8}u_k^{(m)}P_k(x),\ M_6^{\upsilon(m)}(x)=\sum_{k=1}^{8}\upsilon_k^{(m)}P_k(x), \quad (24)$$

where $a_k^{(i)}$, $b_k^{(i)}$, $u_k^{(m)}$ and $\upsilon_k^{(m)}$, $i=1...8,\ m=1\div N_1$ – coefficients of boundary functions of secondary expansions; $P_k(x),\ k=1\div 8$ – fast polynomials [1].

Expressions for coefficients of boundary functions $a_k^{(i)}$, $b_k^{(i)}$, $u_k^{(m)}$, $\upsilon_k^{(m)}$ and fast polynomials $P_k(x)$ look like

$$P_1(x)=\left(1-\frac{x}{a}\right),\ P_2(x)=\frac{x}{a},\ P_3(x)=\left(\frac{x^2}{2}-\frac{x^3}{6a}-\frac{ax}{3}\right),\ P_4(x)=\left(\frac{x^3}{6a}-\frac{ax}{6}\right),$$
$$P_5(x)=\left(\frac{x^4}{24}-\frac{x^5}{120a}-\frac{ax^3}{18}+\frac{a^3x}{45}\right),\ P_6(x)=\left(\frac{x^5}{120a}-\frac{ax^3}{36}+\frac{7a^3x}{360}\right),$$
$$P_7(x)=\left(\frac{x^6}{720}-\frac{x^7}{5040a}-\frac{ax^5}{360}+\frac{a^3x^3}{270}-\frac{2a^5x}{945}\right), \quad (25)$$
$$P_8(x)=\left(\frac{x^7}{5040a}-\frac{ax^5}{720}+\frac{7a^3x^3}{2160}-\frac{31a^5x}{15120}\right),$$

$$a_1^{(i)} = A_i\big|_{x=0},\ a_2^{(i)} = A_i\big|_{x=a},\ a_3^{(i)} = A_i''\big|_{x=0},\ a_4^{(i)} = A_i''\big|_{x=a},\ a_5^{(i)} = A_i^{(4)}\big|_{x=0},$$
$$a_6^{(i)} = A_i^{(4)}\big|_{x=a},\ a_7^{(i)} = A_i^{(6)}\big|_{x=0},\ a_8^{(i)} = A_i^{(6)}\big|_{x=a},\ i = 1..8, \tag{26}$$

$$b_1^{(i)} = B_i\big|_{x=0},\ b_2^{(i)} = B_i\big|_{x=a},\ b_3^{(i)} = B_i''\big|_{x=0},\ b_4^{(i)} = B_i''\big|_{x=a},\ b_5^{(i)} = B_i^{(4)}\big|_{x=0},$$
$$b_6^{(i)} = B_i^{(4)}\big|_{x=a},\ b_7^{(i)} = B_i^{(6)}\big|_{x=0},\ b_8^{(i)} = B_i^{(6)}\big|_{x=a},\ i = 1..8, \tag{27}$$

$$u_1^{(m)} = u_m\big|_{x=0},\ u_2^{(m)} = u_m\big|_{x=a},\ u_3^{(m)} = u_m''\big|_{x=0},\ u_4^{(m)} = u_m''\big|_{x=a},\ u_5^{(m)} = u_m^{(4)}\big|_{x=0},$$
$$u_6^{(m)} = u_m^{(4)}\big|_{x=a},\ u_7^{(m)} = u_m^{(6)}\big|_{x=0},\ u_8^{(m)} = u_m^{(6)}\big|_{x=a},\quad m = 1...N_1. \tag{28}$$

$$\upsilon_1^{(m)} = \upsilon_m\big|_{x=0},\ \upsilon_2^{(m)} = \upsilon_m\big|_{x=a},\ \upsilon_3^{(m)} = \upsilon_m''\big|_{x=0},\ \upsilon_4^{(m)} = \upsilon_m''\big|_{x=a},\ \upsilon_5^{(m)} = \upsilon_m^{(4)}\big|_{x=0},$$
$$\upsilon_6^{(m)} = \upsilon_m^{(4)}\big|_{x=a},\ \upsilon_7^{(m)} = \upsilon_m^{(6)}\big|_{x=0},\ \upsilon_8^{(m)} = \upsilon_m^{(6)}\big|_{x=a},\quad m = 1...N_1. \tag{29}$$

Thus, the boundary value problem (3) – (6) is reduced to the definition $2\left(8+N_1\right)\left(8+N_2\right)$ of unknown coefficients

$$a_k^{(i)},\ b_k^{(i)},\ u_k^{(m)},\ \upsilon_k^{(m)},\ i = 1...8,\ k = 1...8,\ m = 1...N_1,\ a_{n+8}^{(i)},\ b_{n+8}^{(i)},\ u_{n+8}^{(m)},\ \upsilon_{n+8}^{(m)},\ n = 1...N_2. \tag{30}$$

Values of eight coefficients

$$a_1^{(1)},\ b_1^{(1)},\ a_2^{(1)},\ b_2^{(1)},\ a_1^{(2)},\ b_1^{(2)},\ a_2^{(2)},\ b_2^{(2)}, \tag{31}$$

included in (30) are found using the values of the displacement components $U = U(x, y)$ and $V = V(x, y)$ at the corner points of the rectangular region (see formulas (21), (26), (27)). Considering the approval condition (12), the coefficients (31) are determined by the equalities $a_1^{(1)} = b_1^{(1)} = a_2^{(1)} = b_2^{(1)} = a_1^{(2)} = b_1^{(2)} = 0,\ a_2^{(2)} = K\sin 1.2\pi ab,\ b_2^{(2)} = -K\sin a\sin b$.

To find the rest $\left(2\left(8+N_1\right)\left(8+N_2\right)-8\right)$ of the coefficients from (30) we use fast trigonometric interpolation, tested in [3–7]. To do this, we substitute $U = U(x, y)$ and $V = V(x, y)$ from (19) into differential equations (3), (4) and boundary conditions (5), (6). The expressions obtained in this way are not presented in the article because of their cumbersomeness.

From the boundary conditions (5), (6), we obtain linear algebraic equations as follows. We divide the interval $[0, b]$ uniformly by points $y = y_s = sb/\left(N_1+7\right),\ s = 0,1,..,N_1+7$ into N_1+7 segments and write down the equations obtained from the boundary conditions (5) by substituting $U = U(x, y)$ and $V = V(x, y)$ from (19) at each internal calculation point $y = y_s,\ s = 1,..,N_1+6$. We will have $4\left(N_1+6\right)$ linear algebraic equations. Similarly, we divide the interval $[0, a]$ uniformly by points $x = x_s = sa/\left(N_2+7\right),\ s = 0,1,..,N_2+7$ into N_2+7 segments and write down the equations obtained from the boundary conditions (6) by substituting $U = U(x, y)$ and $V = V(x, y)$ from (19) at each internal calculation point $x = x_s,\ s = 1,..,N_2+6$. Thus, we will also have $4\left(N_2+6\right)$ linear algebraic equations.

From differential equations (3), (4) we write linear algebraic equations as follows. On the area of the rectangle, $x \in [0;a],\ y \in [0;b]$ we evenly apply a grid at N_2+8 points $x = x_s = sa/\left(N_2+7\right),\ s = 0,1,..,N_2+7$ and at N_1+8 points $y = y_s = sb/\left(N_1+7\right),\ s = 0,1,..,N_1+7$. To compose a system of linear algebraic equations, only internal points are used, which form a grid of $\left(N_1+6\right)\left(N_2+6\right)$ internal points $\left(x_s, y_s\right)$. Then, when substituting $U = U(x, y)$ and $V = V(x, y)$ from (19) into equations (3), (4), we

write at each calculated point (x_s, y_s). So, we obtain $2(N_1+6)(N_2+6)$ linear algebraic equations. As a result, we arrive at a closed system of $2(N_1+6)(N_2+6)+4(N_1+6)+4(N_2+6)$ linear algebraic equations with respect to the remaining $(2(8+N_1)(8+N_2)-8)$ unknowns from (30). This system of equations is solved in the Maple environment. After that, the found unknowns (30) are substituted into fast expansions (19). Thus, we constructed an approximate analytical solution of the boundary value problem (3) – (6).

The solution of boundary value problems (3), (4), (7) – (10) and (3), (4), (7) – (9), (11) differs from the solution described above only by obtaining linear algebraic equations from the boundary conditions (7) – (10) and (7) – (9), (11). So, when solving a boundary value problem with boundary conditions (7) – (10), coefficients (31) cannot be found in the same way as in a problem with conditions (5), (6). Therefore, to determine them, eight additional calculation points are required (compared to the solution of the above case). Therefore, we divide the interval $[0, b]$ uniformly by points $y = y_s = sb/(N_1+8)$, $s = 0,1,..,N_1+8$ into N_1+8 segments and write down the equations obtained from the boundary conditions (7), (8) by substituting $U = U(x, y)$ and $V = V(x, y)$ from (19) at each internal calculation point $y = y_s$, $s = 1,..,N_1+7$. Thus, we have $4(N_1+7)$ linear algebraic equations. Similarly, we divide the interval $[0, a]$ evenly by points $x = x_s = sa/(N_2+8)$, $s = 0,1,..,N_2+8$ into N_2+8 segments and write down the equations obtained from the boundary conditions (9), (10) by substituting $U = U(x, y)$ and $V = V(x, y)$ from (19) at each internal calculation point $x = x_s$, $s = 1,..,N_2+7$. We will also have $4(N_2+7)$ linear algebraic equations. If mixed boundary conditions (7) – (9), (11) are given, then we find the values of four coefficients from (31) $a_1^{(1)}$, $b_1^{(1)}$, $a_2^{(1)}$, $b_2^{(1)}$ using the values of the displacement components $U = U(x, y)$ and $V = V(x, y)$ at the corner points $(0,0)$ and $(a,0)$: $a_1^{(1)} = b_1^{(1)} = a_2^{(1)} = b_2^{(1)} = 0$, which allows the interval $[0, a]$ to be uniformly divided into N_2+7 segments by points $x = x_s = sa/(N_2+7)$, $s = 0,1,..,N_2+7$ (as in the case of boundary conditions (6)). Thus, to find the remaining four unknowns from (31) $a_1^{(2)}$, $b_1^{(2)}$, $a_2^{(2)}$, $b_2^{(2)}$, we need to divide the interval $[0, b]$ (as in the case of boundary conditions (7), (8)) evenly into N_1+8 segments by points $y = y_s = sb/(N_1+8)$, $s = 0,1,..,N_1+8$.

Results and Discussion

In computational experiments, the number of terms in the Fourier series of the first (19) and second (23) fast expansions is assumed to be the same, i.e. $N_1 = N_2 = N = 3$. As the material of the bar, we choose heavy concrete B30 with the characteristics [24] $E = 32.5 \cdot 10^9$ Pa, $\nu = 0.2$. Then the Lamé coefficients will be equal to $\lambda = 9.03 \cdot 10^9$ Pa, $\mu = 1.35 \cdot 10^{10}$ Pa, and the size of the section will be taken equal to $K = 10^{-6}$, $a = 1$m, $b = 1$ m.

The approximate analytical solution (19) is compared with the exact one (18). The relative error of the stress tensor (2), the residual between the Lamé equilibrium equations (3), (4) and boundary conditions (5) – (11) was calculated by the formula $\delta = |\Delta| / f_{\max} \cdot 100\%$, where Δ is the absolute error, $f_{\max}$ is the maximum value of the object under study.

Let us show the residual δ of the Lamé equilibrium equations (3) and (4) using different boundary conditions in Figs. 1–3.

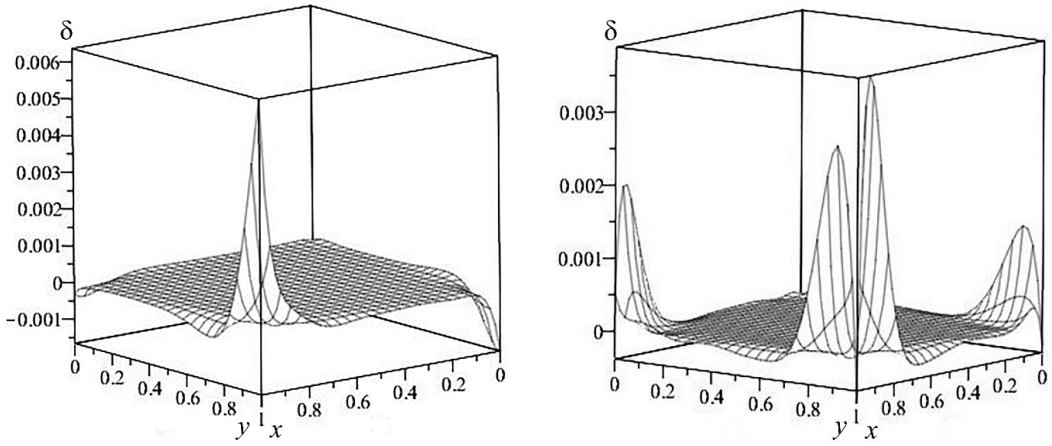

(a) (b)

Fig. 1. Residual δ of the Lamé equilibrium equations under boundary conditions (5), (6): (a) (3), (b) (4)

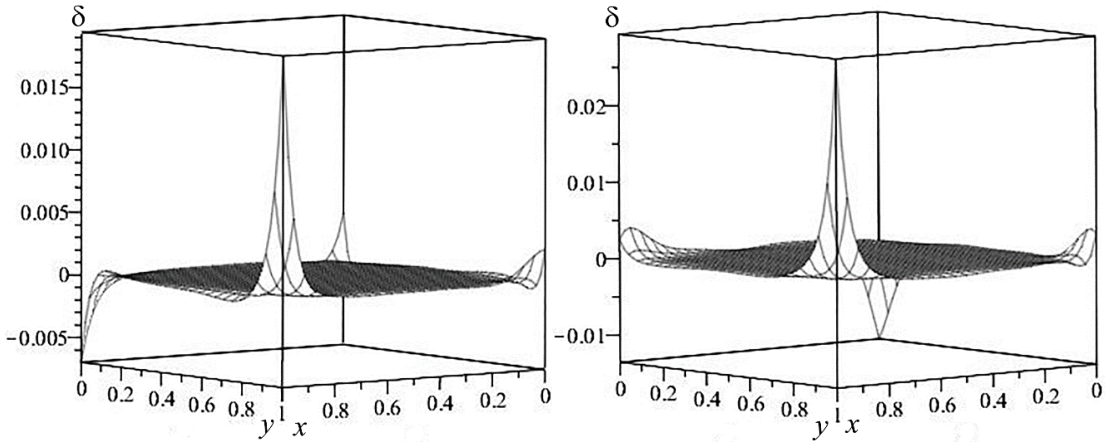

(a) (b)

Fig. 2. Residual δ of the Lamé equilibrium equations under boundary conditions (7) – (10): (a) (3), (b) (4)

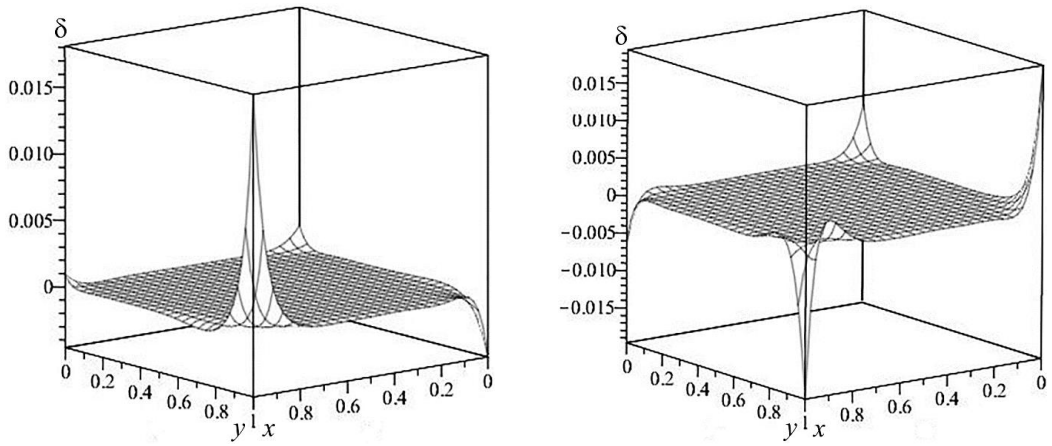

(a) (b)

Fig. 3. Residual δ of the Lamé equilibrium equations under boundary conditions (7) – (9), (11): a) (3), b) (4)

It can be seen from the figures that when boundary conditions (7) – (10) and (7) – (9), (11) are specified, the maximum residual $\delta_{\max}$ of the differential equations will be at the point $(1;1)$. When boundary conditions (5), (6) are specified, the residual $\delta_{\max}$ of the differential equation (3) is also located at the point $(1;1)$, and $\delta_{\max}$ of the differential equation (4) is in its neighborhood on the side $y=1$.

Table 1. Relative error $\delta_{\max}$, %

Object under study		Used boundary conditions		
		(5), (6)	(7) – (10)	(7) – (9), (11)
Tensor Components stresses	σ_{xx}	$4.14\cdot10^{-4}$	$9.87\cdot10^{-4}$	$1.57\cdot10^{-3}$
	σ_{yy}	$4.18\cdot10^{-4}$	$2.19\cdot10^{-3}$	$5.39\cdot10^{-3}$
	σ_{zz}	$3.67\cdot10^{-4}$	$1.05\cdot10^{-3}$	$6.42\cdot10^{-4}$
	τ_{xy}	$3.67\cdot10^{-4}$	$1.53\cdot10^{-3}$	$6.42\cdot10^{-4}$
Residual DE	(3)	$6.34\cdot10^{-3}$	$1.94\cdot10^{-2}$	$1.81\cdot10^{-2}$
	(4)	$3.82\cdot10^{-3}$	$2.93\cdot10^{-2}$	$1.96\cdot10^{-2}$
Residual BC	$U\big\|_{x=a}, U\big\|_{y=b}$	$2.58\cdot10^{-5}$	---	---
	$V\big\|_{x=a}, V_{y=b}$	$5.59\cdot10^{-10}$	---	---
	$U\big\|_{x=0}, V\big\|_{x=0}$	0	---	---
	$U\big\|_{y=0}, V_{y=0}$	0	---	0
	$\sigma_{xx}\big\|_{x=a}$	---	$1.53\cdot10^{-3}$	$1.74\cdot10^{-3}$
	$\sigma_{xx}\big\|_{x=0}$	---	$3.28\cdot10^{-4}$	$1.80\cdot10^{-4}$
	$\tau_{xy}\big\|_{x=a}$	---	$1.17\cdot10^{-3}$	$7.05\cdot10^{-4}$
	$\tau_{xy}\big\|_{x=0}$	---	$1.35\cdot10^{-3}$	$1.78\cdot10^{-3}$
	$\sigma_{yy}\big\|_{y=b}$	---	$1.17\cdot10^{-3}$	$5.50\cdot10^{-3}$
	$\sigma_{yy}\big\|_{y=0}$	---	$1.38\cdot10^{-3}$	---
	$\tau_{xy}\big\|_{y=b}$	---	$1.29\cdot10^{-3}$	$6.91\cdot10^{-4}$
	$\tau_{xy}\big\|_{y=0}$	---	$2.50\cdot10^{-4}$	---

Table 1 lists the values of the maximum relative error $\delta_{\max}$ of the stress tensor components, residuals of differential equations (DE), and residuals of boundary conditions (BC). It can be seen from the table that when using the boundary conditions of three types (1. (5), (6), 2. (7) – (10), 3. (7) – (9), (11)), the solution to the boundary value problem with the Dirichlet conditions is found most accurately. Compared with this problem, the accuracy of determining the components of the stress tensor and the residual of differential equations in two other boundary value problems drops by an order of magnitude. The residual between boundary conditions (7) – (10) and (7) – (9), (11) is inferior in accuracy to the residual between boundary conditions (5), (6) by more than an order of magnitude. It can also be noted that when using any kind of boundary conditions, the components of the stress tensor σ_{xx},

σ_{yy}, σ_{zz}, τ_{xy} are determined by an order of magnitude more accurately than the residuals of the Lamé equilibrium equations (3), (4).

When studying the properties of the stress field in a bar, it is of interest to locate the point with the highest value of stress intensity $\tilde{\sigma}$ [25]:

$$\tilde{\sigma} = \sqrt{\frac{\left((\sigma_{xx}-\sigma_{yy})^2+(\sigma_{yy}-\sigma_{zz})^2+(\sigma_{zz}-\sigma_{xx})^2+6(\tau_{xy})^2\right)}{2}}.$$

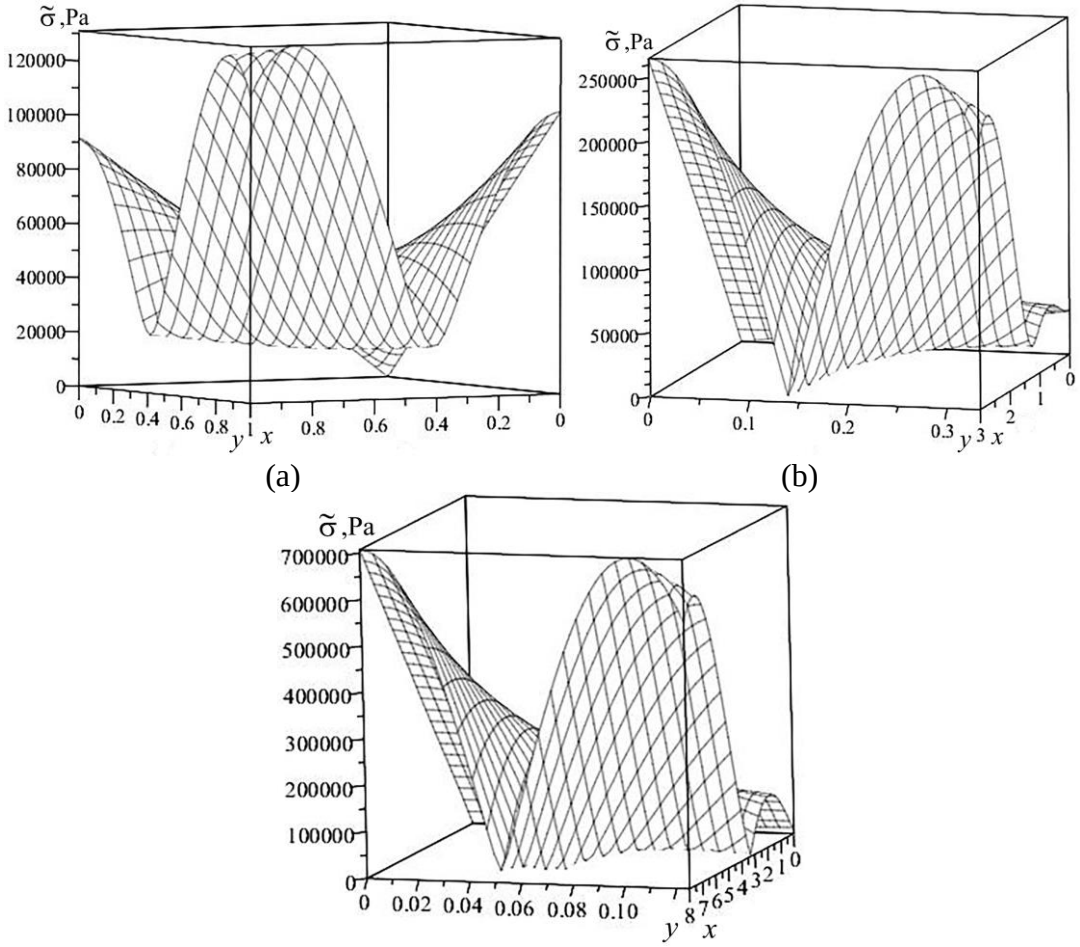

Fig 4. Stress intensity $\tilde{\sigma}$: (a) $a=b=1$, (b) $a=3,\ b=1/3$, (c) $a=8,\ b=1/8$

Let us carry out calculations for three boundary value problems. The stress intensity profiles $\tilde{\sigma}$ will be the same for all types of boundary conditions. In computational experiments, the aspect ratio of the rectangle was chosen in such a way that the cross-sectional area of the bar remained constant. The stress intensity distribution $\tilde{\sigma}$ is shown in Fig. 4. It illustrates that the location of the point with the maximum stress intensity $\tilde{\sigma}_{\max}$ is affected by the aspect ratio of the rectangle. So, for a square section, the point with the maximum stress intensity $\tilde{\sigma}_{\max}$ is located on the side $y=1$ near the corner point $(a;b)$ (Fig. 4(a)), and for a rectangular section $\tilde{\sigma}_{\max}$ it is located either at one point or at two points, depending on the aspect ratio a/b. Thus, at $1<a/b\le 25$ the maximum stress intensity $\tilde{\sigma}_{\max}$ is located at one point $(a;0)$ (Fig. 4(b)), and at $a/b>25$ – at two points (Fig. 4(c)) with

coordinates $(a;0)$ and $(a;0.8b)$. The minimum value of $\tilde{\sigma}_{\min}=0$ is at point $(0;0)$ regardless of the aspect ratio of the rectangle. It can also be concluded from Fig. 4 that among all rectangular sections with different overall dimensions (but the same sectional area), the smallest value of $\tilde{\sigma}_{\max}$ is observed in a bar with a square section.

Conclusions

In conclusion, we note that the solution of the boundary value problem with the Dirichlet conditions is the most accurate of the three considered boundary value problems. Compared with this problem, the accuracy of determining the components of the stress tensor and the residual of differential equations in two other boundary value problems drops by an order of magnitude. The largest residual in the Lamé equilibrium equations is observed in the boundary value problem with given stresses on all sides of the rectangle.

Computational experiments showed that the aspect ratio of the rectangle affects the qualitative form of the stress intensity distribution $\tilde{\sigma}$ and, as a result, the location of points with the maximum stress intensity $\tilde{\sigma}_{\max}$ and their number. At $a/b=1$ the point with $\tilde{\sigma}_{\max}$ is located on the side $y=1$ near the corner point $(a;b)$. For $1<a/b\le 25$ $\tilde{\sigma}_{\max}$ it is at one point $(a;0)$, and for $a/b>25$ it is at two points with coordinates $(a;0)$ and $(a;0.8b)$. The minimum value of $\tilde{\sigma}_{\min}=0$ is at $(0;0)$ regardless of the aspect ratio of the rectangle. Among all rectangular sections with different overall dimensions, but the same sectional area, the smallest value of $\tilde{\sigma}_{\max}$ is observed in a bar with a square section.

References

1. Goloskokov DP, Matrosov AV. Approximate analytical approach in analyzing an orthotropic rectangular plate with a crack. *Materials Physics and Mechanics*. 2018;36(1): 137–141.
2. Kovalenko MD, Menshova IV, Kerzhaev AP, Shulyakovskaya TD. Some solutions of the theory of elasticity for a rectangle. *Mechanics of Solids*. 2021;56(7): 1232–1242.
3. Bogdanov VR, Sulim GT. Plain deformation of elastoplastic material with profile shaped as a compact specimen (dynamic loading). *Mechanics of Solids*. 2013;48(3): 329–336.
4. Aleksandrov VM, Bazarenko NA. The contact problem for a rectangle with stress-free side faces. *Journal of Applied Mathematics and Mechanics*. 2007;71(2): 305–317.
5. Meleshko VV. Thermal stresses in an elastic rectangle. *Journal of Elasticity*. 2011;105(1-2): 61–92.
6. Meleshko VV. Equilibrium of elastic rectangle: Mathieu-Inglis-Pickett solution revisited. *Journal of Elasticity*. 1995;40(3): 207–238.
7. Liu K, Li B. A numerical solution of torsional stress wave propagation in layered orthotropic bar of rectangular cross-section. *International Journal of Solids and Structures*. 2001;38(48–49): 8929–8940.
8. Zhang ZL, Ødegård J, Søvik OP, Thaulow C. A study on determining true stress – curve for anisotropic materials with rectangular tensile bars. *International Journal of Solids and Structures*. 2001;38(26–27): 4489–4505.
9. Franco A, Royer-Carfagni G. Contact stresses in adhesive joints due to differential thermal expansion with the adherends. *International Journal of Solids and Structures*. 2016;87: 26–38.
10. Chernyshov AD, Goryainov VV, Kuznetsov SF, Nikiforova OYu. Application of fast expansions to obtain exact solutions to a problem on rectangular membrane deflection under

alternating load. *Tomsk State University Journal of Mathematics and Mechanics*. 2021;70: 127–142. (In-Russian)
11. Preissner EC, Vinson JR. Application of theorem of minimum potential energy to a complex structure part I: two-dimensional analysis. *International Journal of Solids and Structures*. 2003; 40(5): 1089–1108.
12. Sarychev VD, Nevsky SA, Gromov VE. Theoretical analysis of the stress-deformed state of materials with a gradient structure. *Materials Physics and Mechanics*. 2015;22(2): 157–169.
13. Liu GR, Zhang GY, Wang YY, Zhong ZH, Li GY, Han X. A nodal integration technique for meshfree radial point interpolation method (NI-RPIM). *International Journal of Solids and Structures*. 2007;44: 3840–3860.
14. Smelov VV. Grid version of a nonstandard trigonometric basis and its advantages over a similar polynomial basis. *Numerical Analysis and Applications*. 2014;7: 336–344
15. Isaev VI, Shapeev VP. High-accuracy of the collocations and least squares method for the numerical solution of the Navies-Stokes equations. *Computational Mathematics and Mathematical Physics*. 2010;50(10): 1670–1681.
16. Zaitseva EV, Shmeleva AG, Kazankov VK. Unstable plastic flow in structural materials: time series for analysis of experimental data. *Materials Physics and Mechanics*. 2022;48(2): 208–216.
17. Vasilyev B, Selivanov A. Numerical method of single-crystal turbine blade static strength estimation taking into account plasticity and creep effects. *Materials Physics and Mechanics*. 2019;42(3): 311–322.
18. Annin BD, Bondar V.D, Senashov SI. Group Analysis and Exact Solutions of the Dynamic Equations of Plane Strain of an Incompressible Nonlinearly Elastic Body. *Journal of Applied and Industrial Mathematics*. 2020;14(1): 6–8.
19. Chernyshov AD. Method of fast expansions for solving nonlinear differential equations. *Computational Mathematics and Mathematical Physics*. 2014;54(1): 11–21.
20. Goryainov VV, Popov MI, Chernyshov AD. Solving the stress problem in a sharp wedge-whaped cutting tool using the quick decomposition method and the problem of matching boundary conditions. *Mechanics of Solids*. 2019;54(7): 1083–1097.
21. Chernyshov AD, Goryainov VV, Danshin AA. Analysis of the stress field in a wedge using the fast expansions with pointwise determined coefficients. *IOP Conf. Series: Journal of Physics: Conf. Series.* 2018;973: 012002.
22. Briand T. Trigonometric Polynomial Interpolation of Images. *Image Processing On Line.* 2019;9: 291–316.
23. Porshnev SV, Kusaikin DV. Reconstruction of finite-length periodic discrete-time signals with the use of trigonometric interpolation. *Journal of Instrument Engineering.* 2017;60(6): 504–512.
24. SR 63.13330.2018. *Concrete and reinforced concrete structures. General provisions.* Moscow: Standardinform; 2019.
25. Pisarenko GS, Mozharovsky NS. *Equations and boundary value problems of plasticity and creep*. Kyiv: Nauk. Dumka; 1981.

THE AUTHORS

Chernyshov A.D.
e-mail: chernyshovad@mail.ru

Goryainov V.V.
e-mail: gorvit77@mail.ru

Kovaleva E.N.
e-mail: kovaleva.lena@gmail.com